

Coupling of Monte Carlo and Drift Diffusion Method with Applications to Metal Oxide Semiconductor Field Effect Transistors

Hans KOSINA and Siegfried SELBERHERR

*Institute for Microelectronics, Technical University Vienna,
 Gußhausstraße 27-29, A-1040 Wien, Austria*

(Received August 24, 1990; accepted for publication October 20, 1990)

To describe the electron transport in both the high and low field region of a semiconductor device more accurately a method to couple Monte Carlo and drift-diffusion model has been developed. The space dependent parameters occurring in the drift-diffusion equation are calculated by means of the Monte Carlo method. Their definitions are derived from the Boltzmann transport equation without restricting assumptions about the underlying band structure. With this method regional Monte Carlo device analysis can be performed. The transport coefficients have to be calculated just in the high field region by the computationally demanding Monte Carlo method, thus including non-local effects such as velocity overshoot and ballistic transport, whereas in the remaining regions the solution of the drift-diffusion current relation with local parameters is sufficient.

KEYWORDS: Boltzmann transport, Monte Carlo method, hot electrons, MOSFET, drift-diffusion approximation, silicon, velocity overshoot

§1. Introduction

The electric behavior of monolithic devices which are employed in integrated circuits can only be predicted by means of computer simulation. In many device simulation programs carrier transport is described by the drift-diffusion approximation. However, for present technologies with feature sizes less than one micron, the applicability of the drift-diffusion model becomes questionable. The electric field in the active region of a sub-micron device is often very high and undergoes rapid changes over distances comparable to the mean free path of the carriers. The Monte Carlo method which is based on more accurate physical models is well suited to describe the non-equilibrium transport occurring under these conditions. On the other hand for description of low field transport the drift-diffusion model which uses local transport coefficients provides sufficient accuracy. Moreover, the drift-diffusion model has turned out to be even superior to the Monte Carlo method in regions with retarding fields. Therefore several attempts were published to combine the drift-diffusion and Monte Carlo technique in order to benefit from the different capabilities of both methods.^{1,2)}

§2. Transport Theory

Many semiconductor transport problems can be described by the Boltzmann transport equation. We assume three-dimensional scattering rates in the entire device thus neglecting quantization effects eventually occurring in an inversion layer. Multiplication of the Boltzmann transport equation with wave vector component k_i and integration over \mathbf{k} leads to a momentum balance equation, which reads for electrons

$$-q \left(E_i + \frac{1}{qn} \sum_{j=1}^2 \frac{\partial (n \langle \hbar k_i v_j \rangle)}{\partial x_j} \right) = \langle \int (\hbar k_i - \hbar k'_i) S(\mathbf{k}, \mathbf{k}') d^3 k' \rangle, \quad i=1, 2 \quad (1)$$

where E denotes the electric field, n the electron concentration and v the group velocity. The average operator $\langle A \rangle$ is the mean value of $A(\mathbf{k})$ weighted by the local distribution function $f(x, \mathbf{k})$. The left hand side can be interpreted as driving force that acts on the electron ensemble, consisting of electric field plus diffusion term, whereas the right hand side describes the rate of momentum loss due to scatterings. This equation can be expressed in a form similar to the drift-diffusion current relation. The parameters needed in this current relation are derived in the following way.

For band structures with spheric and ellipsoidal energy surfaces the vector valued momentum loss integral is colinear with the momentum $\hbar \mathbf{k}$

$$\int (\hbar \mathbf{k} - \hbar \mathbf{k}') S(\mathbf{k}, \mathbf{k}') d^3 k' = \hbar \mathbf{k} \lambda_m(E). \quad (2)$$

Here the proportionality factor $\lambda_m(E)$ is the momentum scattering rate. With the local average velocity and the local momentum loss mobility can be defined as

$$\mu = q \frac{\| \langle v \rangle \|}{\| \langle \hbar \mathbf{k} \lambda_m(E) \rangle \|}. \quad (3)$$

This definition does not rely on the relaxation time approximation and, since no effective mass occurs in this formula, extension to general bands is straight forward. In the latter case μ would have tensor property. The definition of the thermal voltage tensor (which is proportional to the temperature tensor $U_{ij} = (k_B/q) T_{ij}$) results directly from the momentum conservation eq. (1)

$$U_{ij} = \frac{1}{q} \langle \hbar k_i v_j \rangle. \quad (4)$$

This definition is independent of the underlying band structure model. Inserting these definitions in eq. (1) we obtain a general current relation

$$J_i = qn\mu \left(E_i + \frac{1}{n} \sum_{j=1}^2 \frac{\partial (n U_{ij})}{\partial x_j} \right). \quad (5)$$

The differences between this current relation and the classical one are twofold. Firstly, the diffusion term is due to the tensor property of the thermal voltage more complicated. Secondly, the parameters μ and U_{ij} can no longer be treated simply as parameters depending on electric field or other local quantities, as it is usually done in the conventional drift-diffusion model, because they carry information of the local distribution function. By means of the Monte Carlo method, which is a tool to solve the Boltzmann transport equation in a stochastic way, we evaluate these parameters. The conventional simulator using the Monte Carlo parameters $\mu(x)$ and $U_{ij}(x)$ in the current relation (5) is then capable of recovering the Monte Carlo results for $n(x)$ and $J_n(x)$. In this way hot electron effects playing an important role in sub-micron devices, such as velocity overshoot and hot carrier diffusion, are consistently included in the conventional simulator. The solution is performed globally in the whole device, but only in the high field region mobility- and temperature profiles have to be extracted from the Monte Carlo procedure. In regions with low fields and low spatial inhomogeneities local models can be used thus saving computation time.

The continuity equation in conjunction with a drift-diffusion current relation employing a scalar temperature yields an elliptic partial differential equation, which has diagonal form. If an anisotropic temperature is taken into account cross derivatives appear in the elliptic operator. Conventional device simulators solve elliptic systems which are in diagonal form. Therefore a scalar temperature is desirable. Neglecting the off diagonal elements in (4) we use a scalar temperature which is the arithmetic mean value of the two main diagonal elements, provided we deal with problems in two space dimensions.

§3. The Semiconductor Model

For the first conduction band of silicon we use a model consisting of six anisotropic valleys with a first order correction for nonparabolicity.³⁾ Acoustic intravalley scattering in the elastic approximation, intervalley phonon scattering, surface roughness scattering and coulomb scattering are taken into account. Except of the latter one all mechanisms are isotropic. In the case of surface scattering in the inversion layer the wave vector is redistributed randomly in a plane parallel to the Si-SiO₂ interface.⁴⁾ For isotropic scattering mechanisms the momentum scattering rate does not differ from the total scattering rate. The following superposition implies independence of all scattering processes

$$\lambda_m(E) = \lambda_{ac}^{tot} + \lambda_{opt}^{tot} + \lambda_{surf}^{tot} + \lambda_{ion}^m. \quad (6)$$

Coulomb interaction is the only one to be treated separately. We evaluate the momentum loss integral (2) with the Brooks-Herring formulation for the transition rate $S(\mathbf{k}, \mathbf{k}')$ and obtain

$$\lambda_{ion}^m(E) = \lambda_{ion}^{tot}(E) - \lambda'_{ion}(E). \quad (7)$$

The subtraction corresponds to the difference of initial and final wave vector in (2). In the following notation β is the reciprocal screening length.

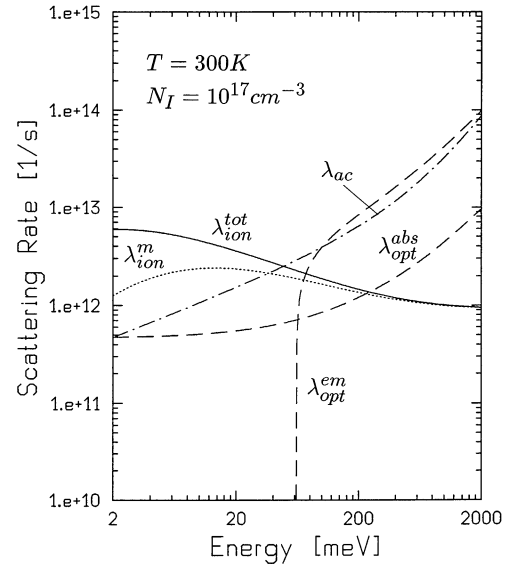


Fig. 1. Total and momentum scattering rates used for mobility calculation.

$$E_\beta = \frac{\hbar^2 \beta^2}{2m_d}, \quad \xi = \frac{2k^2}{\beta^2}. \quad (8)$$

Introducing further shorthands

$$C_{ion} = \frac{N_I q^4}{2^{3/2} \pi \epsilon^2 \sqrt{m_d}}, \quad \gamma(E) = E(1 + \alpha E), \quad (9)$$

the two terms at the right hand side of (7) can be written as

$$\lambda_{ion}^{tot} = \frac{C_{ion}}{E_\beta^2} \sqrt{\gamma(1 + 2\alpha E)} \frac{1}{1 + 2\xi} \quad (10)$$

$$\lambda'_{ion} = \frac{C_{ion}}{8\gamma^2} \sqrt{\gamma(1 + 2\alpha E)} \left(2\xi \frac{1 + \xi}{1 + 2\xi} - \ln(1 + 2\xi) \right). \quad (11)$$

Figure 1 depicts the energy dependencies of total (λ_{ion}^{tot}) and momentum (λ_{ion}^m) scattering rate for ionized impurities, and additionally the total scattering rates for acoustic intravalley phonons (λ_{ac}) and one representative intervalley phonon mode (emission and absorption).

§4. Results

An n-channel MOSFET with $L_{gate} = 0.25 \mu\text{m}$, $t_{ox} = 5 \text{ nm}$ was simulated at room temperature using the combined technique. The device has a metallurgical channel length of $L_{eff} = 0.15 \mu\text{m}$ and exhibits a threshold voltage $U_t = 0.23 \text{ V}$.

For practical simulation of a MOSFET, electrons are injected in source, where they fully thermalize before entering the channel.⁵⁾ In the region of interest, usually near the drain, a sufficiently large number of particles is supplied by a particle split algorithm as proposed in,⁶⁾ thus reducing the statistical uncertainty of the results. The potential distribution in the device was calculated with MINIMOS⁷⁾ under a bias condition of $U_{GS} = U_{DS} = 2.5 \text{ V}$ and $U_{BS} = 0 \text{ V}$.

The two-dimensional distribution of the main diagonal temperatures in the area near the drain are depicted in Fig. 2. The lateral temperature T_{xx} has a maximum value

at the surface, while the maximum of T_{yy} is shifted away from surface. Degradation due to hot electron injection into the oxide can be more accurately modeled by using the spatial distribution of T_{yy} than by using the scalar temperature obtained from average energy. In our simulations the off-diagonal temperatures never exceeded 15% of the main-diagonal elements.

Comparing Figs. 3(a) and 3(b) we see that the large normal field within the inversion layer does not appear in the

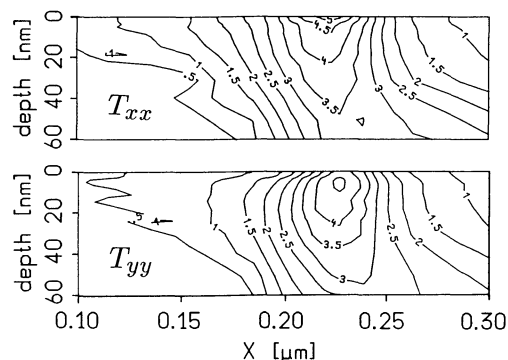


Fig. 2. Lateral and transversal electron temperatures in a quarter micron MOSFET (units [1000 K]).

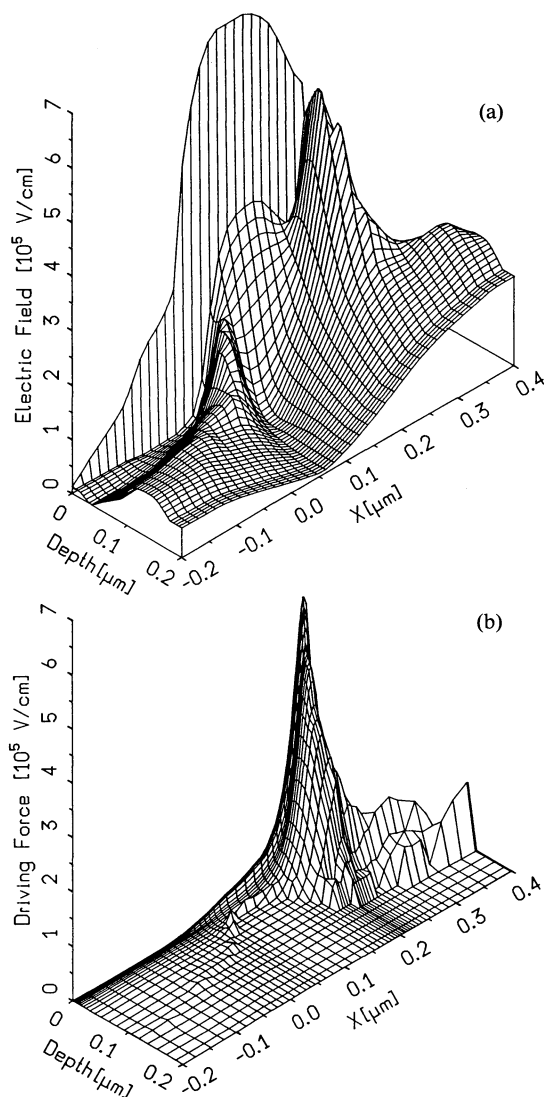


Fig. 3. (a) Electric field and (b) driving force calculated by Monte Carlo in the same device.

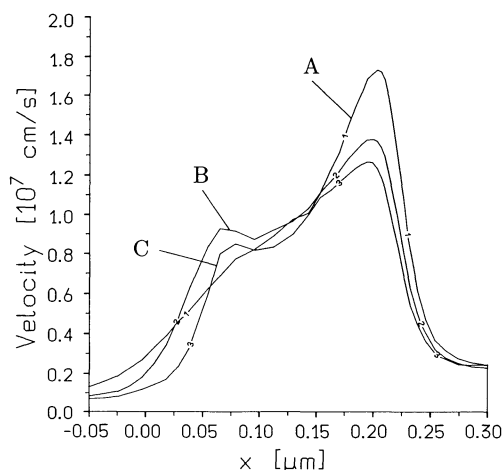


Fig. 4. Electron average velocity along the channel. Curve A: at the Si-SiO₂ interface. Curves B and C: 5 nm and 10 nm away from interface.

driving force. This is obvious since the normal field is compensated by diffusion. The electric field in the source junction is compensated by diffusion as well, since in this area the driving force calculated by Monte Carlo vanishes. The field peak near the drain edge however appears almost unchanged in the driving force, thus accelerating and heating up the electron gas in this area.

Velocity of electrons in the channel is plotted in Fig. 4. The effective channel extends from 0.05 μm to 0.2 μm , the positions of the junctions of source and drain subdiffusion, respectively. In the first half of this range the surface velocity (curve A) is lower than the velocities within the inversion layer since the electrons are pressed towards the surface. Near drain the pressing force has opposite direction and the electron velocity is maximal at the surface. The field peak near drain induces a velocity overshoot of 90% related to the bulk saturation velocity. Comparison of Figs. 3(a) and 3(b) has shown that in the overshoot region diffusion is not important. Therefore velocity overshoot is treated in this model more like a drift phenomenon. It is reproduced by the drift-diffusion current relation (5) by incorporating the nonlocal mobility which will also be increased compared to a local mobility, which cannot produce velocities larger than the bulk saturation velocity.

Acknowledgement

This work is considerably supported by the research laboratories of DIGITAL EQUIPMENT CORPORATION, at Hudson, U.S.A.

References

- 1) S. Bandyopadhyay, M. E. Klausmeier-Brown, C. M. Maziar, S. Datta and M. S. Lundstrom: IEEE Trans. Electron Devices **34** (1987) 392.
- 2) Y. J. Park, D. H. Navon and T.-W. Tang: IEEE Trans. Electron Devices **31** (1984) 1724.
- 3) C. Jacoboni and L. Reggiani: Rev. Mod. Phys. **55** (1983) 645.
- 4) C. Hao, J. Zimmermann, M. Charef, R. Fauquembergue and E. Constant: Solid-State Electron. **28** (1985) 733.
- 5) S. Sangiorgi, B. Ricco and A. Venturi: IEEE Trans. CAD. **7** (1988) 259.
- 6) A. Phillips and P. J. Price: Appl. Phys. Lett. **30** (1977) 528.
- 7) W. Hänsch and S. Selberherr: IEEE Trans. Electron Devices **34** (1987) 1074.